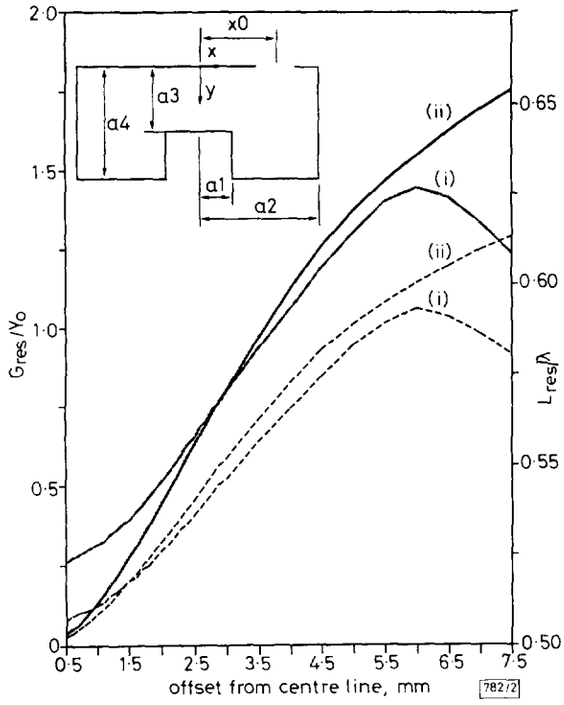

Fig. 2 *Computed resonance length and normalised conductance of longitudinal slot in an array and as an isolated slot in an infinite ground plane, in a single ridge waveguide*

——— slot in array
– – – – isolated slot
a_1 = 1.4mm, a_2 = 8.8mm, a_3 = 2mm, a_4 = 8mm, d = 1.6mm, t = 1mm, g = 20.6mm, f = 7.5GHz

validate the procedure, it is first implemented for the calculation of the infinite longitudinal slot array on the broad walls of conventional rectangular waveguides. Results are compared with those of Yee [6] in Table 1 for l_{res} and G_{res}/Y_0 of the slots, resonating at 9.75GHz in the infinite array model for $\delta\varphi = 0$. The waveguide dimensions are 0.837″ × 0.2″ and the slot width is 0.125″. The thickness t of the waveguide top wall is 0.032″ and the period g of the array is 0.877″. Our computed results agree very well with those of Yee.

For an infinite array of ridged waveguides, computed resonance length and the corresponding slot admittance against offset are shown in Fig. 2. Calculations have been carried out using $N = 1$. In the absence of available data for comparison in the literature, these plots are only shown against reference data for the isolated slot. These plots may be useful for the design of slot arrays in ridged waveguides.

Ackowledgment: The authors are indebted to O. Haluba for bringing the application to their attention. This work was supported in part by the Ramot - Israel Ministry of Industry and Commerce joint fund under contract no. 12875.

18 January 1994
Electronics Letters Online No: 19940396

K. Garb, R. Kastner and R. Meyerova (*Department of Physical Electronics, Faculty of Engineering, Tel Aviv University, Tel Aviv 69978, Israel*)

References

1 KIM, D.Y., and ELLIOTT, R.S.: 'A design procedure for slot arrays fed by single-ridge waveguide', *IEEE Trans.*, 1988, **AP-36**, pp. 1531–1636
2 GREEN, J., SHNITKIN, H., and BERTALAN, P.Y.: 'A symmetric ridge waveguide radiating element for scanned planar array', *IEEE Trans.*, 1990, **AP-38**, pp. 1161–1165
3 ELLIOTT, R.S.: 'An improved design procedure for small arrays of shunt slots', *IEEE Trans.*, 1983, **AP-31**, pp. 48–53
4 SILVESTER, P.P., and FERRARI, R.L.: 'Finite elements for electrical engineers' (New York: Cambridge University Press, 2nd Edn., 1990)
5 JOHNSON, R.C., and JASIK, H.: 'Antenna engineering handbook' (New York: McGraw-Hill, 2nd Edn., 1984), Chap. 9
6 YEE, H.Y.: 'The design of large waveguide arrays of shunt slots', *IEEE Trans.*, 1992, **AP-40**, pp. 775–781

New method for evaluating local pulse wave velocity by measuring vibrations on arterial wall

H. Kanai, K. Kawabe, M. Takano, R. Murata, N. Chubachi and Y. Koiwa

Indexing terms: Biomedical ultrasonics, Biomedical engineering

A new method is proposed for measuring the local pulse wave velocity (PWV), which is an index of the hardness of the aortic wall. Using the method, high spatial resolution, which is necessary in the evaluation of local hardness, is attained.

Introduction: A major concern in the diagnosis of atherosclerosis has been to develop a noninvasive method for evaluating the hardness of the aortic wall. Since the development of the pulse wave velocity (PWV) as an index for use in diagnosis of atherosclerosis [1], numerous studies on measuring the PWV have been reported [2–4]. In the standard method, the PWV is obtained from the difference in the arrival time of pressure waves propagating from the carotid artery to the femoral artery [2, 3].

This method, however, has the following problems:

(i) Because sounds generated by a pressure wave are measured with microphones, the measurable points are limited to those where the aorta exists near the skin surface and the distance between such points is considerable, i.e. several hundred millimetres.

(ii) The measured sound has a frequency component of 10Hz at the most, and the delay time is determined in the time domain. Thus, the spatial resolution of the local evaluation is limited by the wavelength of the pulse wave, that is, several hundred millimetres.

(iii) There is a large increase of the PWV from near the heart to the femoral artery [5]. Thus, the PWV obtained in the standard method between these distant points shows their average value.

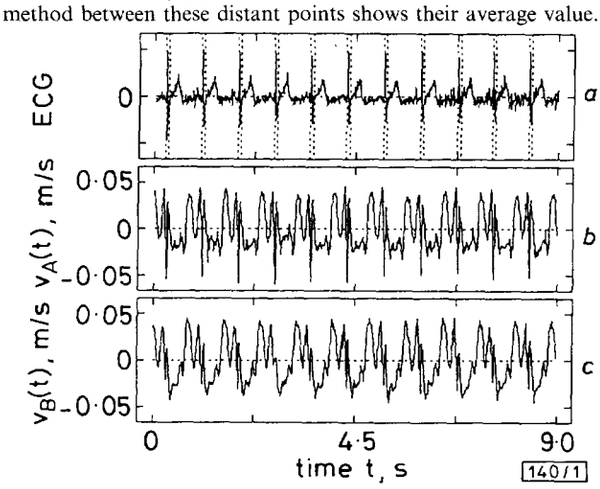

Fig. 1 *ECG and small vibration signals $v_A(t)$ and $v_B(t)$ at the points on the aortic wall near the heart for a young normal person*

a ECG
b $v_A(t)$
c $v_B(t)$
The segments marked by dotted lines around the R-wave in Fig. 1a are analysed in Fig. 4

In the early stage of atherosclerosis, fibrous spots several millimetres in diameter are scattered on the surface of the artery. After

growth of these spots, the arterial wall becomes homogeneously hard in the final stage of atherosclerosis. It is important for early diagnosis, therefore, to measure the local hardness of the surface of the arterial wall. To increase the spatial resolution, it is necessary to measure small vibrations due to pulse waves with higher frequency components.

We have developed a new method to noninvasively measure small vibration signals on the heart wall or the aortic wall from the surface of the skin based on the ultrasonic Doppler effect [6]. In simulation experiments to detect small vibrations with amplitudes of ~50μm on the motion due to heartbeat with an amplitude of 10mm, such signals were successfully detected in the frequency range up to 1kHz [7]. Fig. 1 shows two small vibrations $v_A(t)$ and $v_B(t)$ on the aortic wall near the aortic valve measured from the chest by this method. Frequency components of at least up to 50Hz are involved in these vibration signals. Based on these results, this Letter presents a new method for obtaining local PWV by measuring small vibrations at two points on the aortic wall.

Static experiments using silicon tube: First, by employing a silicon tube as a model of the aorta, the PWV c_0 was obtained from the relationship between the change ΔP in the internal pressure and the change ΔV in the internal volume of the tube as follows [1]:

$$c_0^2 = \frac{V_0}{\rho} \cdot \frac{\Delta P}{\Delta V} \qquad (1)$$

where ρ and V_0 denote the density of water in the tube and the initial volume of the tube, respectively. From the resultant PWV c_0, the Young modulus E is given by

$$E = \frac{2r\rho}{h} c_0^2 \qquad (2)$$

where h and r denote the thickness of the vessel wall and its radius, respectively. They are 2.5 and 7.5mm, respectively, for the employed tube. The effective length of the tube is 840mm and the initial internal volume v_0 is $1.48 \times 10^5 mm^3$. The tube was filled with water and both ends of the tube were clamped. By using a syringe, the volume V and the internal pressure P were simultaneously changed. From the results in Fig. 2, ΔP = 150mmHg and $\Delta V = 6.31 \times 10^3 mm^3$ in the decreasing process of the pressure. Thus, from eqns. 1 and 2, the PWV c_0 and E of the silicon tube are 21.9m/s and 2.87MPa, respectively.

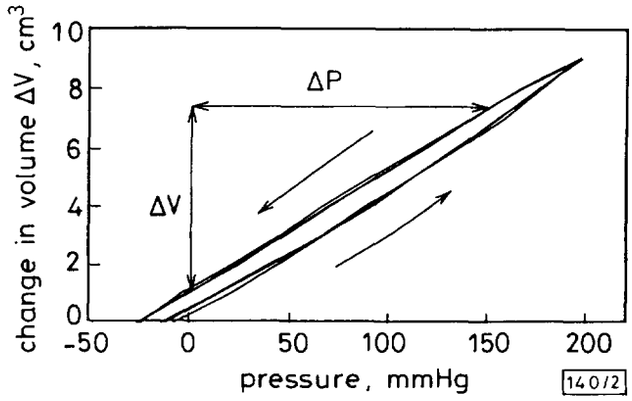

Fig. 2 *Relation between internal pressure P and volume V of tube*

Dynamic experiments using silicon tube: Next, the PWV c_0 of the same silicon tube employed in the above static experiment was measured using an artificial circulation system. In this system, water flowing out of the ventricular-assist device (VAD) goes through the tube, passes a water tank, and finally returns to the VAD. Small vibrations on the tube are simultaneously detected by two acceleration pickups. The distance between them (d_{AB}) is 8.6 mm. Fig. 3*a* and *b* show the two vibration signals measured, $y_A(t)$ and $y_B(t)$, respectively. By applying frequency analysis to the resultant $y_A(t)$ and $y_B(t)$, the coherence function $\gamma^2_{AB}(f)$, and the transfer function, $H_{AB}(f)$, from point A to point B are obtained as shown in Fig. 3*c–e*. Using the delay time τ_{AB} of transmission between points A and B, the phase characteristics $\theta_{AB}(f)$ in Fig. 3*e* of $H_{AB}(f)$ are given by $\theta_{AB}(f) = -2\pi f\tau_{AB}$. Thus, τ_{AB} is determined from the gradient $d\theta_{AB}(f)/df = -2\pi\tau_{AB}$ of $\theta_{AB}(f)$ and then c_0 is given by

$$c_0 = \frac{d_{AB}}{\tau_{AB}} \qquad (3)$$

From the coherence function $\gamma^2_{AB}(f)$, in Fig. 3*c*, these two waves are sufficiently correlated in the frequency range from DC to 700Hz. From the gradient of the phase in the resultant frequency band of Fig. 3*e*, the local PWV c_0 is determined to be 22.4m/s. From eqn. 2, the Young modulus E is 3.01MPa. These values almost coincide with those obtained in the former static experiment. Therefore, it is confirmed that the local hardness of the vessel wall is evaluated with high spatial resolution by measuring two small vibrations on the vessel wall.

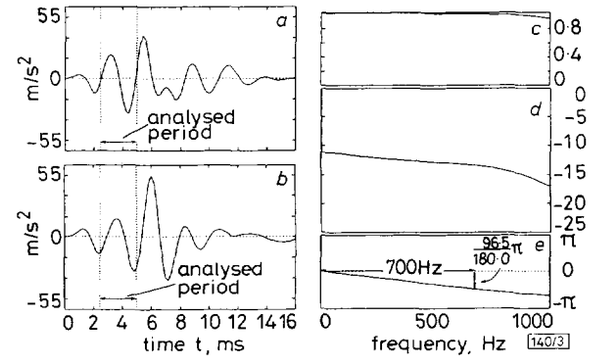

Fig. 3 *Vibration signals $y_A(t)$ and $y_B(t)$, and coherence function $\gamma^2_{AB}(f)$ between them, and phase characteristic $\angle H_{AB}(f)$ of the transfer function $H_{AB}(f)$ from $y_A(t)$ to $y_B(t)$*

a $y_A(t)$
b $y_B(t)$
c γ^2_{AB}
d $|H_{AB}|$ [dB]
e θ_{AB} [rad]

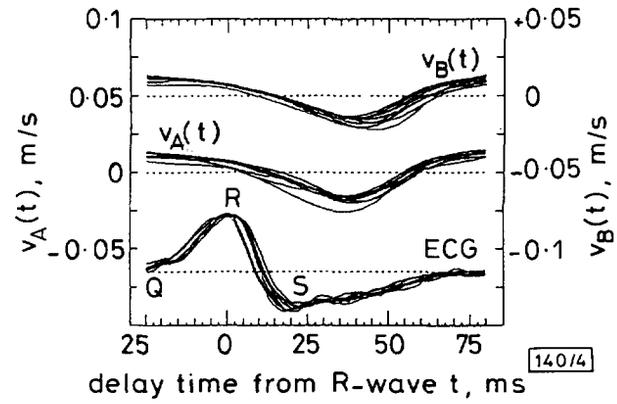

Fig. 4 *Segments of the ECG and the small vibration signals $v_A(t)$ and $v_B(t)$ around the R-wave of the ECG for 11 beat periods in Fig. 1*

In vivo experiments: We applied the procedure in the above dynamic experiments to the two vibration signals $v_A(t)$ and $v_B(t)$ simultaneously measured at the two points on the aortic wall in Fig. 1*b* and *c*. As shown in Fig. 4, there is evident time delay of ~2.66ms from $v_A(t)$ to $v_B(t)$ around the R-wave of the ECG in each beat period. As the distance between the two points d_{AB} is 9.1 mm, the PWV c_0 is obtained as 3.4m/s.

Conclusions: By the proposed method, the measured vibration signals have frequency components of up to ~50Hz and delay time is determined in the frequency domain. Thus, the spatial resolution achieved by the proposed method is several millimetres, which almost coincides with the size of the fibrous spots on the arterial wall in the early stage of atherosclerosis. Therefore, the proposed method will be effective for local evaluation of the hardness on the aortic wall.

16 February 1994
Electronics Letters Online No: 19940393

H. Kanai, K. Kawabe, M. Takano, R. Murata, and N. Chubachi (*Department of Electrical Engineering, Tohoku University, Aramaki-aza-Aoba, Aoba-ku, Sendai 980, Japan*)

Y. Koiwa (*School of Medicine, First Department of Internal Medicine, Tohoku University, Amamiyacho, Sendai 980, Japan*)

References

1 BRAMWELL, J.C., and HILL, A.V.: 'The velocity of the pulse wave in man', *Proc. Roy. Soc. B.*, 1922, **93**, pp. 298–306

2 HALLOCK, P.: 'Arterial elasticity in man in relation to age as evaluated by the pulse wave velocity method', *Arch. Int. Med.*, 1934, **54**, pp. 770–798

3 HASEGAWA, M.: 'A fundamental study on human aortic pulse wave velocity', *Jikeikai Medical J.*, 1970, **85**, pp. 742–760

4 LEHMANN, E.D., GOSLING, R.G., FATEMI-LANGROUDI, B., and TAYLOR, M.G.: 'Non-invasive Doppler ultrasound technique for the *in vivo* assessment of aortic compliance', *J. Biomech. Eng.*, 1992, **14**, pp. 250–256

5 MCDONALD, D.A.: 'Blood flow in arteries' (London, Edward Arnold, 1974)

6 KANAI, H., SATOH, H., HIROSE, K., and CHUBACHI, N.: 'A new method for measuring small local vibrations in the heart using ultrasound', *IEEE Trans.*, 1993, **BE-40**, (12), pp. 1233–1242

7 KAWABE, K., KANAI, H., and CHUBACHI, N.: 'Accuracy evaluation in ultrasonic-Doppler-based measurement of small vibrations for acoustical diagnosis of the aortic wall', *Electron. Lett.*, 1993, **29**, (10), pp. 915–916

Novel pseudo-class AB fully differential 3V switched current system cells

H. Träff and S. Eriksson

Indexing terms: Switched-current circuits, Circuit design

A novel pseudo-class AS low conductance fully differential switched current memory structure with high clock feedthrough (CFT) attenuation, is presented. It is designed with a 3V power supply. An integrator using the proposed structure is also presented with simulation results.

Introduction: Mobile telecommunications is a very active area of research. The 'one-chip'-concept with low power and low power supplies (battery) has been aimed for, making analogue circuit techniques compatible with inexpensive digital processes. This may require current mode circuit techniques [1] that have the potential for high frequency operation, mixed analogue digital design, small area and power consumption. A low voltage mode dynamic range also contributes to the advantages over voltage mode circuits. Switched current techniques (SI) [2] seem a promising alternative to switched capacitor techniques (SC). However, SI still suffers from 'childhood diseases' such as clock feedthrough errors (CFT), finite output/input conductance ratio etc. CFT is by far the most severe, and several papers have been published on the topic [2–5]. Here, low conductance operation and fully differential structures are used to overcome some of the problem.

In this Letter we present a novel fully differential structure for one of the most important SI building blocks, the memory circuit (MC) [2, 6]. It is crucial to have good MCs to design high performance SI system level blocks as delay lines, integrators, filters, A/D and D/A convertors, etc, and the simulation performance of an integrator is also shown. The circuits are currently under fabrication.

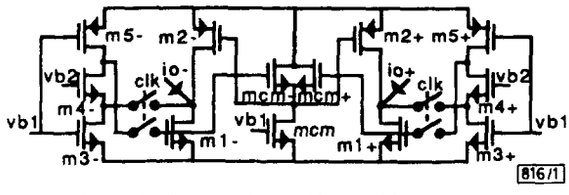

Fig. 1 *Novel pseudo-class AB fully differential low power SI structure*

Input and output signals at *io+* and *io–*

Memory circuit: The novel fully differential memory circuit is shown in Fig. 1. The second generation structure [2] has been used to avoid transistor mismatch. Because both M1 and M2 adjust to match the input current in clock phase 1 and a small quiescent current flows, the action may be considered as class AB. However, the connection of M2+ and M2– to the common mode feedback (CMFB) circuitry MCM, MCM+, MCM–, give the devices a slightly different task. Now, the M2 transistors will regulate and memorise only the common mode part of the signal, whereas the M1 transistors take care of both common and differential mode parts. This structure is advantageous also because it uses only one switch for both M1 and M2. The CFT attenuation is thereby increased by a factor 2 [6]. Another pair of switches are included to separate the output from the discharging nodes of the M4 devices in clock phase 2. Furthermore, the specific structure allows the gate-source voltages of M1 and M2 to be designed to operate with low conductances. This results in large gate-source voltages, meaning that the signal dependent CFT becomes relatively smaller and the signal dependent error on the output is reduced. The large gate-source voltages, however, do result in large signal independent CFT [6]. Fully differential structures effectively reduce common mode offsets, and the signal independent CFT presents itself as a positive constant on both the positive and negative side.

The stages M3 – M5 perform the two actions of keeping the output voltage constant, and transferring and amplifying the small signal voltage at the input to the gates of M1 and MCM transistors; thus

$$v_{g,d} \simeq \frac{i_i}{g_{m,1}} \quad v_{g,c} \simeq \frac{i_i}{g_{d,5}}$$

$$\text{where } g_{m,1} \simeq g_{m,2},\ g_{m,i} \gg g_{d,j}\ \forall i,j$$

where $v_{g,d}$ and $v_{g,c}$ are the differential and common mode voltages at the drain of M4 (node g) in the input phase, respectively. g_m and g_d are the transconductances and output conductances. Passive common gate transistors M4+ and M4– are sufficient for this task.

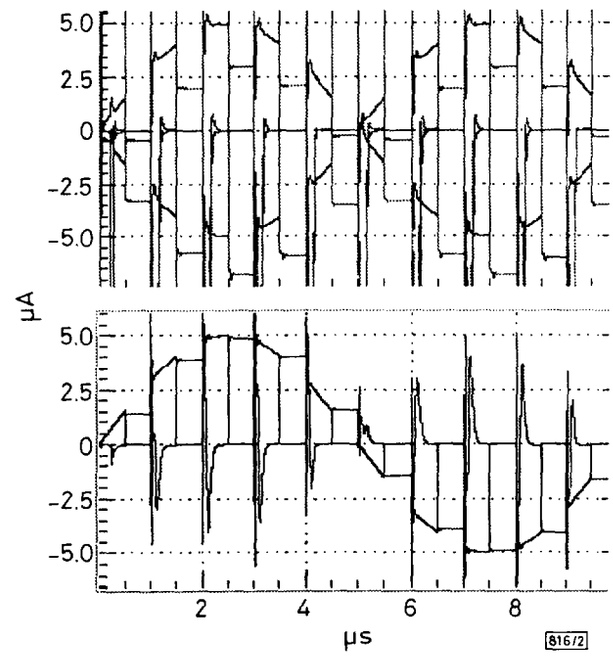

Fig. 2 *Track- and -hold simulation of pseudo-class AB fully differential SI memory circuit*

The first diagram shows the positive and negative single differential input and output signals respectively (inputs are sine-shpaed and outputs S&H-shaped). The large CFT is obvious, but due to the specific structure it is equal and constant. This results in the small CFT in the lower diagram, which shows $(i_{in+} - i_{in-})/2$ and $(i_{out+} - i_{out-})/2$, respectively. The large spiking due to recharging of amplifier internal nodes is easily seen.

For a single memory circuit, a smaller problem remains to be solved. Because the M3 – M5 structure is disconnected during one half clock cycle, the drain and source nodes of M4 devices discharge slightly. The result is that when the structure is connected